International Journal of Latest Research in Engineering and Technology (IJLRET)
ISSN: 2454-5031
www.ijlret.com || Volume 04 - Issue 09 || September 2018 || PP. 25-32

The Controlled Human Gyroscope – Virtual Reality Motion Base Simulator

Randy C. Arjunsingh[1], Matthew J. Jensen[1], Razvan Rusovici[2], Ondrej Doule[3]
[1](*Mechanical and Civil Engineering Department, Florida Institute of Technology, United States)*
[2](*Aerospace, Physics and Space Sciences Department, Florida Institute of Technology, United States)*
[3](*Computer Engineering and Sciences Department, Florida Institute of Technology, United States)*

Abstract: Flight motion simulators are currently used for flight training and research, but there are many limitations to these existing systems. This paper presents a low-cost design for a rotational motion platform titled, 'The Controlled Human Gyroscope'. It uses a 4-axis system instead of the conventional 3-axis system to avoid gimbal lock and prevent the unnecessary motion of the user. The Human Gyroscope features unlimited rotation about the roll, pitch and yaw axes regardless of the occupant's orientation. It will therefore provide high fidelity motion simulation and if it is paired with a translational motion platform, it can provide up to 6 degrees of freedom. Equations of motion for this specific system are presented in this paper and can be used to develop a control algorithm.

Keywords: Flight motion simulator, Gimbal lock, Human gyroscope, Full rotational control, Rotational Motion

I. INTRODUCTION

Motion simulation provides a cheap and safe alternative to field training. It submerges the operator into a virtual environment and synchronizes this virtual motion with actual movement of the operator. Mistakes in the field can therefore be avoided, situations can be more accurately replicated than in static simulators and dangerous training situations in real-world no longer have consequences, as they are not in an actual aircraft. Overall training cost of pilots or astronauts is reduced significantly since operation and maintenance of a simulator is cheaper than that of an actual vehicle. Less risk is involved while operating a motion platform than a spacecraft or aircraft, so insurance and liability costs are significantly reduced and higher fidelity training in virtual environment ensures better learning and training results.

The Human-Centered Design Institute at Florida Institute of Technology proposed developing an adaptive spaceship cockpit motion simulator. Its purpose was to serve as a low fidelity rotational motion simulator to simulate human space flight. It needed to expose the human body to three-dimensional rotational motion like the NASA human gyroscope that was originally designed to train astronauts. Unlike NASA's gyroscope, the vision of the project was to develop a device that would have independently controlled, unlimited rotation, about all axes and would fit in office environment. The Human Gyroscope needed to actively and independently control each axis of rotation in order to replicate roll, pitch and yaw in any given orientation. With a modular cockpit, different air or space crafts can be portrayed, therefore creating environments that are congruent to the actual vehicle or aerospace flight profile / trajectory without restrictions. While this rotational motion platform was designed specifically to simulate spaceflight, there are many other uses.

Advanced and aggressive flight simulation can be conducted on this system. Most existing dynamic flight simulators have limited rotational motion making them inadequate in reproducing extreme flight situations. Even simple fixed wing Private Pilot training exercises such as steep turns and stalls are difficult to mimic on limited motion simulators. The angles that the system has to roll, pitch or yaw are simply too much for the simulator to replicate. Unusual attitude recovery is an important part of a pilot's training. Situations arise in flight where visual flight rules are no longer applicable. Such situations include flying: through clouds, at night or in inclement weather. Unusual attitudes occur in these situations because the pilot is unable to use visual cues to determine their orientation. The pilot's vestibular system may perceive (based on other stimuli like balance, acceleration and gravity) the aircraft in straight and level flight, but this is not always the case. The aircraft could be in a completely different orientation than assumed by the pilot and dangerous situations can arise. The human gyroscope can be used for training, while providing a safe, no consequence environment for the operator in nominal office environment.

Spatial disorientation is a contributing factor in many aviation accidents [1]. The main factors that contributed to the conceptualization of this project is space motion sickness, microgravity adaptation syndrome and disorientation. Piloted tasks such as docking maneuvers and reentry or extravehicular tasks can be compromised due to space motion sickness [2]. Motion simulators can be used as preventative action for motion

sickness and spatial disorientation as well as training to mitigate and recover vehicle during off-nominal or emergency situations. Stroud et al indicates that preflight training in virtual reality devices that can closely replicate spacecraft movement will reduce the incidence and/or severity of motion sickness and disorientation. A person's spatial awareness is determined by his/ her position, orientation and external objects like buildings and other people. On earth, gravity and visual cues are the basis for determining orientation. In certain conditions, such as spaceflight, these stimuli become unreliable or unavailable [2]. When external visual reference factors and gravity are removed, vision (de-coupled from un-stimulated vestibular system) becomes the primary method for perceiving orientation and may provide conflicted information compare to what human body is used to in gravity-driven environment on Earth [3]. Nonetheless, a person can be trained to adapt to these unfamiliar situations by undergoing e.g., motion simulator training [4].

There is certainly a need to better understand human-system interaction and integration of vehicle interfaces in human spaceflight, especially for microgravity environment . A pilot or astronaut's comfort can be studied from the perspective of cognitive and physical ergonomics such as their body support to specific interaction controllers or information and input devices displacement. Models of the cockpits can be used in the simulator and tested to approve controllers and display placement and prove or disprove their effectiveness. Since modern aircrafts exhibit stick fixed stability using hydraulic actuation devices, they are required to have force feedback systems. Operator interactions with the control and feedback system can also be studied using a motion simulator. Simply examining these cases in a static environment is only half of what needs to be done. Frequently analyzing and surveying pilots in dynamic simulation devices can provide crucial, emergent information about the new requirements on the cockpit systems architecture, design and placement of controls and other operator-system interaction issues.

II. LIMITATIONS OF EXISTING SYSTEMS

Many motion simulators use the Stewart Platform as its source for motion. The Stewart Platform (or hexapod) is a parallel device that consists of a platform supported by six telescoping hydraulic or electronic struts [5]. The platform is moved by changing the length of the telescoping struts. Changing the length of one strut causes a realignment of all the struts which allows the platform to have six degrees of freedom [5]. While this does provide six degrees of freedom, its motion envelope is still very limited, typically to less than 45 degrees of roll, pitch and yaw.

Limited motion is one of the issues phasing simulators today. Many simulators have a limited range of motion and those that do offer unlimited rotation faces the issue of gimbal lock. Gimbal lock or kinematic singularity occurs when two of the three axis of a rotational system are driven into a collinear configuration. This results in the loss of one degree of freedom [6]. The user therefore loses either pitch, roll or yaw. In order to achieve a high fidelity device, the system must be able to avoid gimbal lock. While a 3-axis system can be controlled in such a way as to try to avoid these locking positions, the fidelity of the system is lost because the operator will undergo unnecessary movement while the system attempts to avoid locking positions. Fig 1 is a drawing of a 3 degree of freedom gimbaled system where the green ring controls pitch, the red ring controls yaw and the blue ring controls roll. If the simulator is oriented as shown in Fig2, for example, a 90-degree roll in a spacecraft, one degree of freedom is lost. In this case, roll is duplicated and pitch is lost.

Figure 1: Typical three degree-of-freedom gimbal system

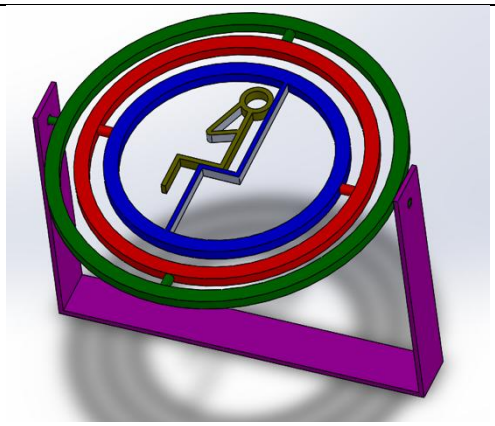

Figure 2: Common three degree-of-freedom gimbal lock situation

The only way to completely avoid gyroscope lock is to use a 4-axis device. In a 4-axis gimbal, one of the axes of rotation is redundant to another. In this system, since all four axes are controlled individually, they can be moved to always avoid gyroscope lock. It does this while maintaining the fidelity of the system by not moving the operator unnecessarily. Washout filters are used in limited motion simulators to return the simulator to a neutral position while moving at an acceleration lower than the level of human perception [7]. When fast pace, constantly changing maneuvers need to be simulated, a washout algorithm is unable to keep up. One of the engineering solutions to simply add a fourth ring to the 3-ring human gyroscope, at a cost of increasing the requirements on size of the facility. Adding a fourth ring for simulation, while also able to accommodate one pilot and 200kg of hardware, would require a non-standard building with a high ceiling. Therefore, a hybrid (rings plus toothed wheel) technical solution was selected.

III. DESIGN AND METHODOLOGY

The major tasks of the Controlled Human Gyroscope were to mimic a spacecraft's launch, landing, reentry, atmospheric flight and microgravity flight. The operator should have unlimited rotation about the roll, pitch and yaw axes at any given time and hence avoid gimbal lock.

The most basic form of the proposed design is derived from a spinning disc gyroscope. While the design looks similar to an Aerotrim, the functionality is very different. Instead of being physically powered by a human, every axis is individually controlled by hydraulic motors. The controlled human gyroscope has four gimbals, and therefore four degrees of rotational freedom, where one is redundant to avoid gimbal lock. Fig 3 is a 3D drawing of the developed Human Gyroscope without its internal components. The operator will be seated in the inner ring (blue) and each ring will control an axis of rotation.

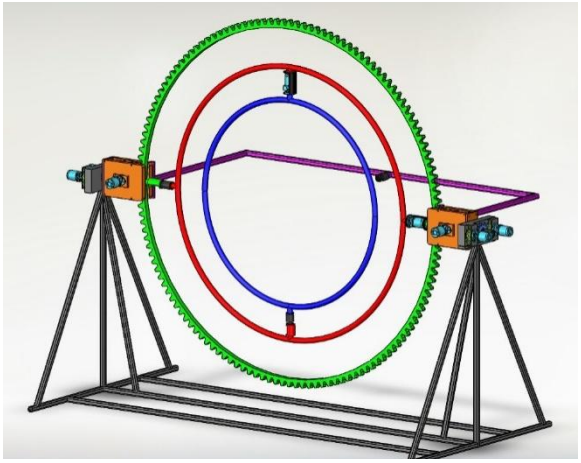

Figure 3: 3D drawing of the proposed design for a fully controllable gyroscope simulator

Most motion simulators have a limited range in replicating roll, pitch and yaw. Those that are capable of continuous rotation about every axis are likely to encounter gimbal lock. As mentioned before, gimbal lock occurs when two axes of rotation become collinear. When this happens, rotating any one of those axes will

produce the same motion (either roll, pitch or yaw). One degree of freedom is therefore forfeited or in other words, the operator has lost one of his/ her rotation axes. Depending on which two axes line up, the operator will no longer be able to either roll, pitch or yaw them. It is important for gimbal lock to be avoided to maintain a high fidelity simulation. Fig 4 is a drawing of a four degree of freedom system in a gimbal lock configuration. In this instance, the simulator is replicating a 90-degree roll as seen above in Fig 2. Similarly to the three DoF gimbals, pitch is lost here as well.

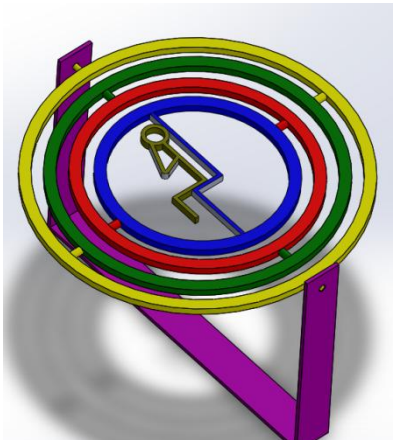

Figure 4: Four degree-of-freedom gimbal lock situation

The only way to combat gimbal lock with the three DoF system is to use special motion cueing algorithms with washout filters. These filters help the system return to a neutral position or in other words, return to an orientation where roll, pitch and yaw can be simulated. As discussed before, this results in unnecessary movement of the operator and the algorithm may not be able to follow along with aggressive simulation. The four DoF gimbals possess the exact same properties as the design used in this project. Software on the system will detect when a potential gimbal lock situation is approaching and instead of moving to a neutral location, the fourth axis will move to avert this problem. Fig 5 shows how the motion simulator will move to maintain control of roll, pitch and yaw. The green ring now controls pitch, the red ring controls yaw, the blue ring controls roll and yaw is duplicated with the yellow axis.

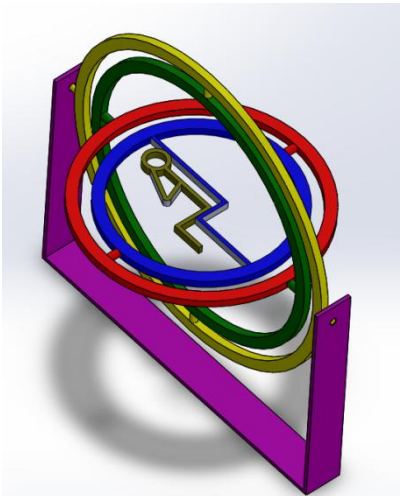

Figure 5: Alternate four degree-of-freedom gimbal lock solution

IV. KINEMATIC ANALYSIS

4.1. Mathematical description of gimbal lock

As flight technology advances, spacecrafts and aircrafts become very maneuverable. Older aircrafts had gravity fed fuel systems that restricted the maneuverability of that plane significantly. If the plane banks excessively, fuel would be cut off to the engine causing it to stall. Modern aircrafts have fuel pumps and baffled fuel tanks that remove rotational limitations of the aircraft. Once the plane is structurally capable, it will have

unlimited rotation about its axes. Complicated out of plane maneuvers such as barrel rolls, lag rolls, displacement rolls and spirals, just to name a few, are part of aerobatics and military flight training and dates back to the early 1900's. A three degree-of-freedom system will encounter kinematic singularities while trying to replicate this type of motion. An example of a three degree of freedom gimbal is shown in Fig 6.

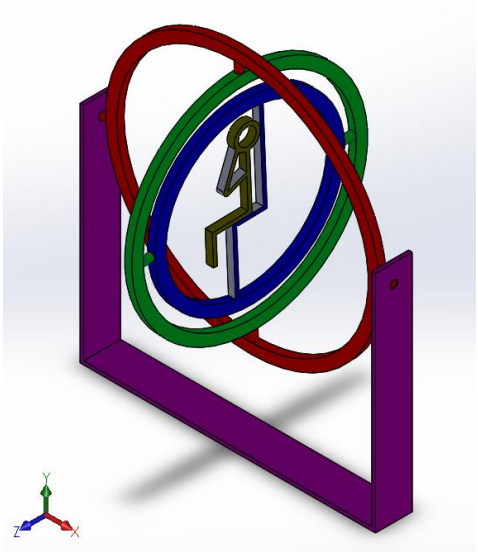

Figure 6: Drawing showing three degree-of-freedom gimbal system

In order to mathematically explain gimbal lock or kinematic singularity, Fig 6 will be referenced. An inertial frame has been set up where the positive y-axis points up, the positive x-axis points to the right and the positive z-axis points out of the paper. Each gimbal has its own frame of reference attached to it that rotates with that gimbal (body fixed reference frame). With the orientation in Fig 6, the outer gimbal rotates about the x-axis (pitch), the middle gimbal rotates about the y-axis (yaw) and the inner gimbal rotates about the z-axis (roll). In this orientation, the gimbal frames are all aligned with the inertial frame since this is the starting position. Rotation about any axis in this system can be converted from the inertial frame using a transformation matrix. The transformation matrices are given as:

$$R_x(\delta_1) = \begin{bmatrix} 1 & 0 & 0 \\ 0 & \cos(\delta_1) & \sin(\delta_1) \\ 0 & -\sin(\delta_1) & \cos(\delta_1) \end{bmatrix} \quad (1)$$

$$R_y(\delta_2) = \begin{bmatrix} \cos(\delta_2) & 0 & -\sin(\delta_2) \\ 0 & 1 & 0 \\ sin(\delta_2) & 0 & \cos(\delta_2) \end{bmatrix} \quad (2)$$

$$R_z(\delta_3) = \begin{bmatrix} \cos(\delta_3) & sin(\delta_3) & 0 \\ -sin(\delta_3) & \cos(\delta_3) & 0 \\ 0 & 0 & 1 \end{bmatrix} \quad (3)$$

Where δ in these matrices are rotation angles and the subscripts describe which axis it is attached to.

The final transformation matrix from the inertial frame to the gimbal frame, used to convert velocity and acceleration vectors, is the product of the previous three matrices:

$$T_{Transform} = R_z(\delta_3) * R_y(\delta_2) * R_x(\delta_1) \quad (4)$$

Substituting the transformation matrices in equations 1, 2, and 3:

$$T_{Transform} = \begin{bmatrix} \cos(\delta_3)\cos(\delta_2) & \sin(\delta_3)\cos(\delta_1) + \cos(\delta_3)\sin(\delta_2)\sin(\delta_1) \\ -\sin(\delta_3)\cos(\delta_2) & \cos(\delta_3)\cos(\delta_1) - \sin(\delta_3) * \sin(\delta_2)\sin(\delta_1) \\ \sin(\delta_2) & -\cos(\delta_2)\sin(\delta_1) \end{bmatrix}$$

$$\begin{matrix} \sin(\delta_3)\sin(\delta_1) - \cos(\delta_3)\sin(\delta_2)\cos(\delta_1) \\ \cos(\delta_3)\sin(\delta_1) + \sin(\delta_3)\sin(\delta_2)\cos(\delta_1) \\ \cos(\delta_2)\cos(\delta_1) \end{matrix}\Bigg] \quad (5)$$

The transpose of matrix $T_{Transform}$ can be used to convert kinematic motions from the body fixed frame to the inertial frame. Euler angles are used to describe the attitude of the body fixed frame with respect to the inertial frame. The kinematic motion for the gimbals are determined by computing the inverse of the mapping matrix from Euler angle rates to body rates [8]. For the 3-axis gimbal shown in Fig 6, the Euler angle rates to body rates are given by:

$$\omega_{body}^{body} = R_z(\delta_3) * R_y(\delta_2) * R_x(\delta_1) * \left[\dot{\delta}_1, 0, 0\right]^T + R_z(\delta_3) * R_y(\delta_2) * \left[0, \dot{\delta}_2, 0\right]^T + R_z(\delta_3) * \left[0, 0, \dot{\delta}_3\right]^T \quad (6)$$

Substituting equations 1, 2 and 3 into 6:

$$\omega_{body} = \begin{bmatrix} \cos(\delta_2).\cos(\delta_3) & \sin(\delta_3) & 0 \\ -\cos(\delta_2).\sin(\delta_3) & \cos(\delta_3) & 0 \\ \sin(\delta_2) & 0 & 1 \end{bmatrix} \begin{bmatrix} \dot{\delta}_1 \\ \dot{\delta}_2 \\ \dot{\delta}_3 \end{bmatrix} \quad (7)$$

Where ω_{body} is the body angular rate with coordinates in the body fixed reference frame [8]. We can then take the inverse of this matrix and use it to find the required gimbal rates. We will denote the rate vector by $\dot{\gamma}$ and the matrix by A:

$$\omega_{body} = A * \dot{\gamma} \quad (8)$$

$$\dot{\gamma} = A^{-1} * \omega_{body} \quad (9)$$

$$A^{-1} = \frac{1}{det\,(A)} * adjoint(A) \quad (10)$$

$$A^{-1} = \frac{1}{\cos(\delta_2)} * \begin{bmatrix} \cos(\delta_3) & -\sin(\delta_3) & 0 \\ cos(\delta_2).\sin(\delta_3) & cos(\delta_2).\cos(\delta_3) & 0 \\ -cos(\delta_3).\sin(\delta_2) & sin(\delta_3).\sin(\delta_2) & \cos(\delta_2) \end{bmatrix} \quad (11)$$

This inverse of A, like any other matrix, only exists if the determinant of A is non-zero. The determinant of A (stated above) is $\cos(\delta_2)$. The inverse of A therefore does not exist where $\cos(\delta_2)$ is equal to zero. This occurs when $\cos(\delta_2)$is $n\pi/2$, where n= ±1,±3… . At these values of δ_2, the system encounters gimbal lock. Referring to Fig 6, if δ_2 is $\pi/2$ or 90 degrees, the red ring rotates 90 degrees about the y-axis making the rings concentric and the system loses pitching motion.

4.2. The four axis system

A flying machine traveling through space has six degrees-of-freedom, three of which are rotational. Simulating the attitude of these vehicles can be done with a 3-axis gimbal, but certain attitudes will cause this to encounter gimbal lock. A four-axis system was proposed that, if controlled correctly, would avoid kinematic singularity with its redundant gimbal. Creating an algorithm to control this system is a very complex process and not in the scope of this project, but equations of motion will be proposed. These equations can then be transferred to software that can solve the equations and incorporate these solutions in a control algorithm for the system.

Methods for solving these equations have been presented and one example of that is seen in the paper by Wang *et. al*. [9]. Wang proposed that for a direct kinematic manipulator, a dual Euler method can be used to solve the expression of attitude angles. For inverse kinematics, a pseudo-inverse gradient projection method is used to obtain optimal velocity solution.

Referring to Fig 7, the axes of rotation have been labeled 1 to 4 from the outer to inner gimbal respectively. An inertial frame has been set up where the positive y-axis points up, the positive x-axis points to

the right and the positive z out of the paper. Similarly to above, the subscripts of δ describe which axis and gimbal it is attached to. Rotation about any axis in this system can be converted to the gimbal frame using a transformation matrix. The transformation matrices are given as:

$$R_x(\delta_1) = \begin{bmatrix} 1 & 0 & 0 \\ 0 & \cos(\delta_1) & \sin(\delta_1) \\ 0 & -\sin(\delta_1) & \cos(\delta_1) \end{bmatrix} \quad (12)$$

$$R_z(\delta_2) = \begin{bmatrix} \cos(\delta_2) & sin(\delta_2) & 0 \\ -sin(\delta_2) & \cos(\delta_2) & 0 \\ 0 & 0 & 1 \end{bmatrix} \quad (13)$$

$$R_x(\delta_3) = \begin{bmatrix} 1 & 0 & 0 \\ 0 & \cos(\delta_3) & \sin(\delta_3) \\ 0 & -\sin(\delta_3) & \cos(\delta_3) \end{bmatrix} \quad (14)$$

$$R_y(\delta_4) = \begin{bmatrix} \cos(\delta_4) & 0 & -\sin(\delta_4) \\ 0 & 1 & 0 \\ sin(\delta_4) & 0 & \cos(\delta_4) \end{bmatrix} \quad (15)$$

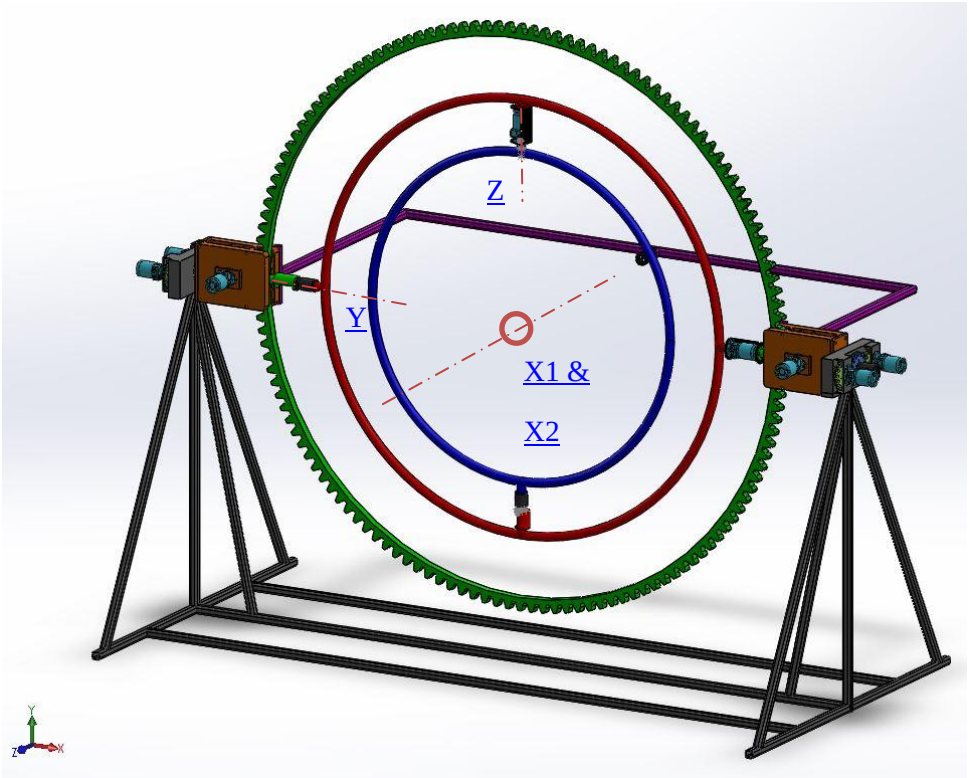

Figure 7: Drawing of the full four-axis motion simulator with inertial coordinate system

Like the three-axis system, a final transformation matrix from the inertial frame to the gimbal frame can be computed. In this case, the rotation sequence is: $R_y(\delta_4), R_x(\delta_3), R_z(\delta_2), R_x(\delta_1)$. The complete transformation matrix is given by:

$$T_{Transform} = R_y(\delta_4) * R_x(\delta_3) * R_z(\delta_2) * R_x(\delta_1) \quad (16)$$

$$T_{Transform} = \begin{bmatrix} \cos(\delta_4)\cos(\delta_2) - \sin(\delta_4)\sin(\delta_3)\sin(\delta_2) \\ -\cos(\delta_3)\sin(\delta_2) \\ \sin(\delta_4)\cos(\delta_2) + \cos(\delta_4)\sin(\delta_3)\sin(\delta_2) \end{bmatrix}$$

$$\cos(\delta_1) * [\cos(\delta_4)\sin(\delta_2) + \sin(\delta_4)\sin(\delta_3)\sin(\delta_2)] + \sin(\delta_4)\cos(\delta_3)\sin(\delta_1)$$
$$\cos(\delta_3)\cos(\delta_2)\cos(\delta_1) - \sin(\delta_3)\sin(\delta_1)$$
$$\cos(\delta_1) * [\sin(\delta_4)\sin(\delta_2) - \cos(\delta_4)\sin(\delta_3)\cos(\delta_2)] - \cos(\delta_4)\cos(\delta_3)\sin(\delta_1)$$

$$\begin{matrix} \sin(\delta_1) * [\cos(\delta_4)\sin(\delta_2) + \sin(\delta_4)\sin(\delta_2)\cos(\delta_2)] - \sin(\delta_4)\cos(\delta_3)\cos(\delta_1) \\ \cos(\delta_3)\cos(\delta_2)\sin(\delta_1) + \sin(\delta_3)\cos(\delta_1) \\ \sin(\delta_1) * [\sin(\delta_4)\sin(\delta_3) - \cos(\delta_4)\sin(\delta_3)\cos(\delta_2)] + \cos(\delta_1)\cos(\delta_4)\cos(\delta_3) \end{matrix}\Bigg] \quad (17)$$

For the four-axis gimbal shown in Fig 7, the Euler angle rates to body rates are given by:

$$\omega_{body}^{body} = R_y(\delta_4) * R_x(\delta_3) * R_z(\delta_2) * R_x(\delta_1) * [\dot{\delta_1}, 0, 0]^T + R_y(\delta_4) * R_x(\delta_3) * R_z(\delta_2) * [0, 0, \dot{\delta_2}]^T + R_y(\delta_4) * R_x(\delta_3) * [\dot{\delta_3}, 0, 0]^T + R_y(\delta_4) * [0, \dot{\delta_4}, 0]^T \quad (18)$$

$$\omega_{body}^{body} = \begin{bmatrix} \cos(\delta_4)\cos(\delta_2) - \sin(\delta_4)\sin(\delta_3)\sin(\delta_2) & -\sin(\delta_4)\cos(\delta_3)\cos(\delta_4) & 0 \\ -\cos(\delta_3)\sin(\delta_2) & \sin(\delta_3) & 0 \\ \sin(\delta_4)\cos(\delta_2) + \cos(\delta_4)\sin(\delta_3)\sin(\delta_2) & \cos(\delta_4)\cos(\delta_3) & \sin(\delta_4) \end{bmatrix} \begin{matrix} 1 \\ 0 \\ 0 \end{matrix} \begin{bmatrix} \dot{\delta_1} \\ \dot{\delta_2} \\ \dot{\delta_3} \\ \dot{\delta_4} \end{bmatrix} \quad (19)$$

V. CONCLUSION

The Controlled Human Gyroscope in this paper had unlimited rotation about all three axes. It used a redundant gimbal making it a four-axis system that successfully avoided gimbal lock unlike the conventional three-axis setup. Complex maneuvers like those performed by military and aerobatic pilots can be easily reproduced on this system.

Flight motion simulators, according to literature, has to provide high fidelity motion cues or the simulators can have a negative effect on the users when they transition to actual aircrafts. The Controlled Human Gyroscope with a suitable control algorithm will be able to accurately perform these motion cues without the unnecessary movement of the user since it is able to avoid gimbal lock. A high fidelity simulator such as this one will provide more accurate research and training capabilities.

REFERENCES

[1]. Nooij, S. A. E., Groen, E. L., Rolling into Spatial Disorientation: Simulator Demonstration of the Post-Roll (Gillingham) Illusion, *Aviation Space and Environmental Medicine, 82(5),* 2011, 505-512.

[2]. Stroud, K. J., Harm, D. L., and Klaus, D. M., Using Virtual Reality for Predicting and Preventing Space Motion Sickness, *Proceedings of the 54th International Astronautical Congress of the International Astronautical Federation, the International Academy of Astronautics, and the International Institute of Space Law*, Bremen, Germany, 2003.

[3]. Chen, W., Chao, J. G., Wang, J. K., Chen, X. W., and Tan, C., Subjective Vertical Conflict Theory and Space Motion Sickness,*Aerospace Med Hum Perform*., *87(2)*, 2016, 128-136

[4]. Lawson, B. D., Rupert, A. H., and McGrath, B. J., The Neurovestibular Challenges of Astronauts and Balance Patients: Some Past Countermeasures and Two Alternative Approaches to Elicitation, Assessment and Mitigation, *Frontiers in Systems Neuroscience*,*10*, 2016, 1-96.

[5]. Van Silfhout, R. G., High-Precision Hydraulic Stewart Platform,*Review of Scientific Instruments, 70(8)*, 1999, 3488-3495.

[6]. Jie, M.A., Qinbei, X. U., Four-axis gimbal system application based on gimbal self-adaptation adjustment, *Proceedings of the 34th Chinese Control Conference*, Hangzhou, China, 2015.

[7]. Chen, S. H., Fu, L. C., An Optimal Washout Filter Design with Fuzzy Compensation for a Motion Platform, *IFAC Proceedings Volumes, 44(1)*, 2011, 8433-8438.

[8]. Carter, D. R., Duffey, P., Bachorski, S., Kägi, M., Havlicsek, H., Weighted least-squares based control for a four axis gimbal set, *Proceedings of SPIE Defense, Security, and Sensing*, Orlando, Florida United States of America, 2010.

[9]. Wang, X.C., Zhao, H., Ma, K.M., Huo, X., and Yao, Y., Kinematics analysis of a novel all-attitude flight simulator, *Science China Information Sciences, 53(2)*, 2010, 236–247.